JOURNAL OF THEORETICAL
AND APPLIED MECHANICS

ONLINE FIRST

DESIGN AND EXPERIMENT OF MEMBRANE-TYPE ACOUSTIC METAMATERIALS USED IN EMUs TO CONTROL LOW FREQUENCY NOISE

Peng LIU[1], Hao LIN[2], Pan GAO[1], Pengyi TIAN[1], Chengcheng JIANG[1], Leiming SONG[2*], Xiaoqing DONG[1]

[1] *Locomotive & Car Research Institute, China Academy of Railway Sciences Corporation Limited, Beijing 100081, China*
[2] *School of Mechanical, Electronic and Control Engineering, Beijing Jiaotong University, Beijing 100044, China*
[*]corresponding author, *lmsong@bjtu.edu.cn*

Acoustic metamaterials, a new type of material with great design flexibility, have been widely studied by scholars in recent decades. For high-speed electric multiple units (EMUs), a membrane-type acoustic metamaterial is used to design a lightweight sound insulation material that adapts to the space requirements within the low frequency range. A theoretical analysis on the membrane-type acoustic metamaterial was carried out. The sound insulation coefficient was calculated. Experimental comparisons were conducted on six different thicknesses of films combined with five types of additional masses. The experimental results verified the sound insulation performance. It has great potential for designing lightweight noise reduction structures.

Keywords: membrane-type acoustic metamaterials; high-speed electric multiple units; low frequency noise; experiment.

1. Introduction

With the increase of train speed, the problem of noise becomes more and more serious. In order to solve the noise problem inside high-speed electric multiple units (EMUs), a large number of control measures are adopted in the design process.

According to the traditional method of sound insulation quality, it is observed that doubling the material mass results in only a 6 dB increase in sound insulation, making it relatively easy to achieve high-frequency sound wave insulation. There are three main types of commonly used sound insulation methods. The first involves using double-layer boards with air or vacuum sandwiched in between to enhance sound reflection and block sound wave propagation for improved insulation. However, this approach increases volume and does not provide ideal acoustic performance for low-frequency bands. The second method entails plate reinforcement to control stiffness and enhance material's sound insulation properties, but it does not effectively control low-frequency noise (Jung *et al.*, 2019). The third method is to lay damping materials or sound-absorbing materials on the surface of panels, which slows down panel structure vibration to achieve the noise reduction function. However, this method increases the structural mass and size and has certain limitations when used under space constraints.

The sound insulation design of the high-speed EMUs primarily incorporates the aforementioned methods, including the utilization of double-layer board materials for vehicle cross-section structure, optimization of vehicle body structure profile parameters, and enhancement of damping for profile and interior panels. Sound insulation treatments are implemented for critical noise sources such as interior flooring (e.g., aluminum honeycomb panels) and traction converter

equipment compartments (Lu *et al.*, 2016; Thompson *et al.*, 2015). Nevertheless, components like interior flooring entail high costs, substantial mass, and intricate designs, resulting in inconvenient maintenance. Furthermore, in order to fulfill the demands for light-weighting, energy efficiency, environmental preservation, and reduction of environmental contamination in vehicles, compromises are made with regards to acoustic design. This leads to a decline in sound insulation performance and presents novel challenges for noise control within the train. Hence, there is a necessity to develop a lightweight structure capable of achieving sound insulation effects (Ho *et al.*, 2003).

The emergence of acoustic metamaterials provides a new approach for the design of low-frequency noise control structures. The localized resonance units (Assouar *et al.*, 2016; Fang *et al.*, 2006) or other characteristic units (Song *et al.*, 2015) contained in acoustic metamaterials can generate extraordinary physical properties such as negative refraction and negative mass density, which offer new solutions to the challenges faced by traditional sound insulation materials in low-frequency sound insulation (Jena *et al.*, 2019; Wang *et al.*, 2019). Liu *et al.* (2000) proposed the concept of local resonant phononic crystals, which used small-sized structures to regulate low-frequency and long-wavelength mechanical waves (Sheng *et al.*, 2003). This design broke through the limitations imposed by traditional laws of mass and created a band gap in the low-frequency range, preventing the propagation of sound waves and providing new ideas for low-frequency vibration and noise control (Ma *et al.*, 2014; Rostami-Dogolsara *et al.*, 2020). In recent years, membrane-type acoustic metamaterials (MAMs) have become hot topics, opening up new chapters for the realization and application of lightweight low-frequency sound insulation materials (Ahluwalia *et al.*, 1985; Kriegsmann *et al.*, 1984).

Research on MAMs can be divided into studies on the acoustical vibration characteristics of thin film structures with or without additional mass. Naify *et al.* (2011; 2012) from the University of Southern California, studied different combinations of thin film unit structures with single or multiple masses added to them, comparing different sound insulation characteristics using the finite element results and impedance tube test results. The results show that this structure had over a five-fold improvement in sound insulation compared to traditional methods, forming multiple peaks at lower frequencies to broaden the soundproofing frequency band. Zhang *et al.* (2013) studied the low-frequency sound insulation performance of thin film acoustic metamaterials with different qualities attached to adjacent units, which was elaborated from both the experimental and finite element aspects. The results show that when the total mass remains unchanged, the film structure with different masses can form multiple sound insulation peaks, and the sound insulation effect is better than that of the film structure with the same mass.

On the other hand, research on MAMs often involves combining thin films with other structures without additional mass. Zhou *et al.* (2019) designed a combination structure of EVA perforation and PI film to study how structural parameters and material parameters affect sound insulation effects. The structure showed improved sound insulation effects within the frequency range of 80 Hz–800 Hz (Zhou *et al.*, 2019; Yoshizawa *et al.*, 2019). Although good sound insulation effects can be achieved with various additional masses or other combined structures, these structures have higher manufacturing costs which are not conducive to practical engineering applications.

The purpose of this article is to study the application of film-type acoustic metamaterials in low-frequency vibration characteristics and propose a method for designing sound insulation structures to address low-frequency noise problems during the operation of high-speed trains. In this article, structural design of the MAMs was conducted, and the characteristic theoretical analysis was carried out in Section 2. The experiment was carried out to verify sound insulation performance of MAMs in Section 3.

This study has the following contributions: the proposed structure consists of a rigid frame, elastic membrane, and additional mass, which form a high sound insulation area in the low-frequency range through local resonance of the unit, thereby achieving sound insulation effects

in this frequency range. Compared with traditional design solutions, this structure is lighter and more compact, providing new ideas for lightweight sound insulation and noise reduction designs for high-speed trains.

2. Structural design and theoretical analysis

The study shows that the interior of train compartment mainly experiences noise generated by wheel-rail excitation during operation (Varanasi *et al.*, 2013; Thompson *et al.*, 2006). As the bogies are distributed at both ends of the train compartment, when the train is running on a straight track, the interior noise exhibits a characteristic where the sound pressure level is greater at the end of the car than in the middle section. The frequency domain characteristics of these two areas of noises are not significantly different.

When the EMUs is traveling at high speed, Fig. 1a demonstrates the comparison of noise spectrum between the end and middle areas of the carriage. It indicates a high energy concentration in the middle and low frequency bands. Specifically, the noise is predominantly distributed within the range of 125 Hz to 2000 Hz. The identification results of interior noise sources indicate that most of them concentrate on floor areas in end sections as shown in Fig. 1b.

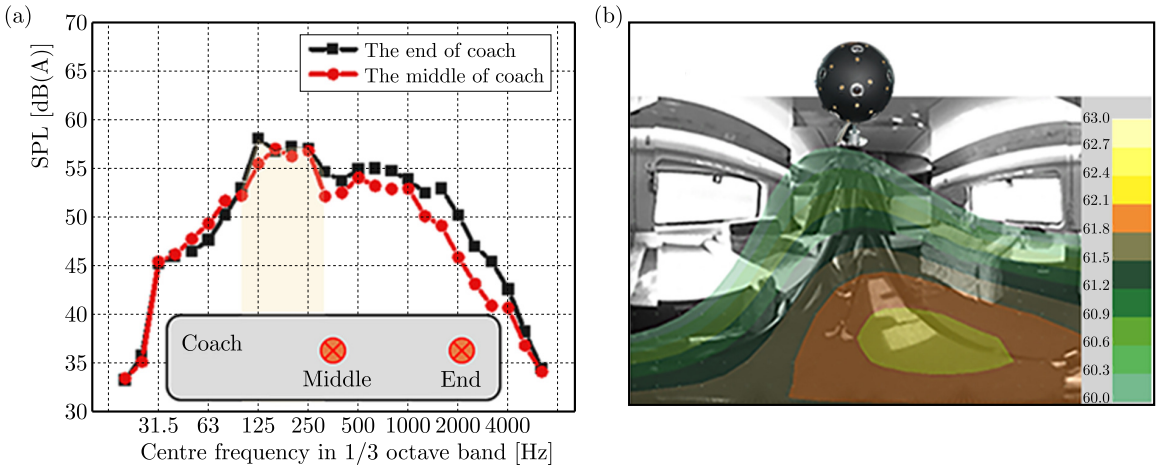

Fig. 1. Noise characteristics inside the EMUs: (a) noise characteristics at the end and middle of the carriage; (b) sound source distribution diagram at the end of the carriage.

According to sound insulation mass laws, achieving good sound insulation effects using traditional methods would require materials with dimensions much larger than those available in the vehicle design space for this frequency range. Therefore, composite materials and structures are used for design purposes; however, this method conflicts with lightweight design concepts and may result in decreased sound insulation effects after weight reduction. The development of MAMs provides a solution to address these issues by utilizing their structural features which can meet design space requirements while achieving good sound insulation effects.

In order to create desired structures, an analysis is conducted on acoustic vibration characteristics of MAMs first. When the thin-film acoustic metamaterial is fixed in the acoustic impedance tube for test measurement, the main distribution state of the internal sound pressure is shown in Fig. 2a. Figure 2b illustrates one type of circular MAMs where orange represents a membrane with radius R_1 and black represents additional mass with radius R_2. To simplify the model, this paper considers the case of vertically incident unit plane waves and focuses on the steady-state response of thin film structures.

For sound waves in a circular tube, rigid boundary conditions are satisfied with zero air velocity at the wall. Due to the symmetry of the structure and acoustic pressure load, only axisymmetric modes of the thin film structure need to be considered.

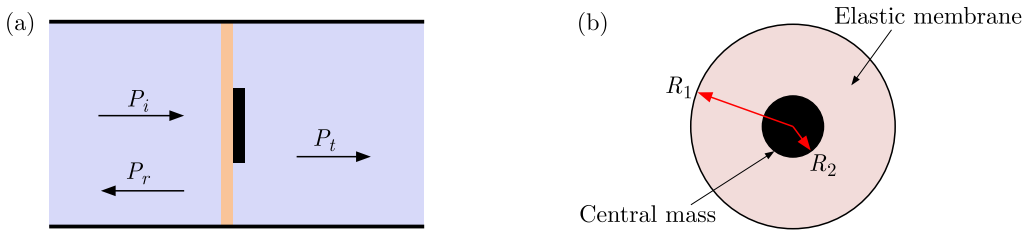

Fig. 2. (a) Schematic diagram of plane wave incident acoustic wave tube; (b) schematic of circular MAMs.

The annular membrane vibrates under acoustic loading as following equation:

$$\Delta P = P_i + P_r - P_t, \tag{2.1}$$

where transmitted sound pressure is P_t, incident sound pressure is P_i, reflected sound pressure is P_r.

In the cylindrical coordinate system, the incident sound pressure is formed by the incident wave and the reflected wave, and is expressed as

$$p_i + p_r = e^{-j\mathbf{k}_a z} + \sum_{n=0}^{\infty} R_n J_0(\mathbf{k}_n r) e^{j\sqrt{\mathbf{k}_a^2 - \mathbf{k}_n^2} z}, \tag{2.2}$$

where J_0 is zero-order Bessel function, $\mathbf{k}_n$ is wave vector, R_n is reflection coefficient, $\mathbf{k}_a$ is wave vector in the air.

Transmitted sound pressure is expressed as follows:

$$p_t = \sum_{n=0}^{\infty} T_n J_0(\mathbf{k}_n r) e^{-j\sqrt{\mathbf{k}_a^2 - \mathbf{k}_n^2} z}, \tag{2.3}$$

where T_n is the transmitted coefficient.

In a circular impedance tube, the propagation of sound pressure satisfies the wave equation. The velocity of the rigid boundary is zero. The continuity condition is that the normal vibration velocity of the air is continuous with the normal vibration velocity of the film.

Since the stiffness of the central mass block is much greater than that of the thin film, its motion can be described by the rigid body translation displacement. The thin film acts as a spring for the central mass, providing a restoring force F.

From the aforementioned analysis, two vibration control equations of the MAMs can be obtained. The first equation is the vibration equation under the acoustic pressure ΔP as follows:

$$-\rho_1 \omega^2 \eta_1 - T\nabla^2 \eta_1 = \Delta p, \tag{2.4}$$

where the surface density of the elastic film is ρ_1, and the transverse vibration displacement under the action of tension T is η_1.

Due to the symmetry of structure and the sound pressure load, the central mass is regarded as a rigid body displacement η_2. Then the motion equation of the mass block is shown in the second vibration control equation:

$$-\pi R_2^2 \omega^2 \rho_2 \eta_2 = \iint \Delta p dS_2 - F, \tag{2.5}$$

where the surface density of the central mass is ρ_2, and the restoring force of the film acting on the central mass is F.

The acoustic transmission coefficient of the structure can be obtained by means of the modal superposition method. The structural vibration displacement can be expressed as

$$\eta(r) = \sum_{m=1} W_m(r) q_m. \tag{2.6}$$

Combined with boundary conditions and continuity conditions, the equation is as follows:

$$p_i - p_r = p_t = j\omega\rho_a c_a \eta, \tag{2.7}$$

where ρ_a and c_a are density and sound speed of air, respectively.

Only a plane wave can propagate to the far field, the far field transmission coefficient is determined by surface displacement of the structure as follows:

$$t_P = |\rho_a c_a \omega \langle\eta\rangle| = \left|\rho_a c_a \omega \frac{\int \eta dS}{S}\right|. \tag{2.8}$$

The sound insulation coefficient is expressed by the following formula:

$$\mathrm{STL} = 20\log_{10}(1/t_P). \tag{2.9}$$

According to Eq. (2.9), the sound insulation coefficient curve of the structure is calculated, as shown in Fig. 3.

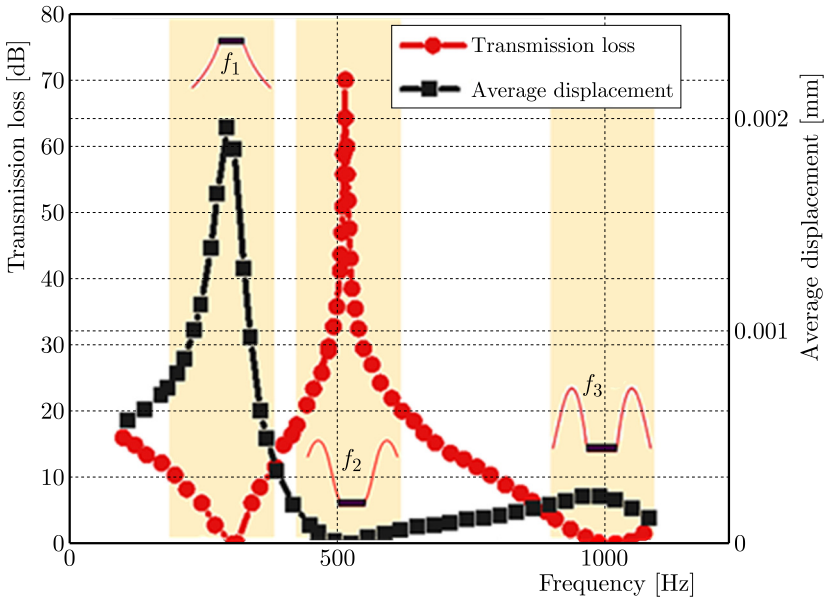

Fig. 3. Structure sound insulation curve and surface mean displacement curve.

In Fig. 3, the small figure is the modal shape of the structure at corresponding frequency points. At the resonance frequency points (f_1, f_3), the sound insulation quantity is very small. It can be seen from Eq. (2.8) that the transmission coefficient is related to the average displacement η of the structure. According to the mean displacement curve, there is a significant displacement of the structure itself at resonance, which means that the sound waves continue to propagate through the structure. When the sound insulation peak occurs at f_2 point, the average displacement of the structure is close to 0, which can be regarded as a rigid body which greatly enhances structural sound insulation performance and reduces the sound transmission coefficient. Therefore, it can be concluded that by adjusting parameters such as radius and surface density of additional mass as well as surface density of thin films, one can design structural sound insulation coefficients accordingly.

3. Experimental analysis

In order to further verify acoustic characteristics under different parameters for this structure, different thicknesses of thin films along with small masses with different sizes and weights are prepared for testing purposes, as shown in Figs. 4a and 4b. By using the acoustic impedance tube to test these structures, the experimental results were compared with calculated results, as shown in Fig. 4c. The presence of additional mass in the composite film structure results in a higher sound insulation performance compared to pure film structures. This is mainly due to the change in modal behavior and the emergence of new axisymmetric modes caused by the presence of additional mass. It also leads to a larger equivalent mass when anti-resonance occurs.

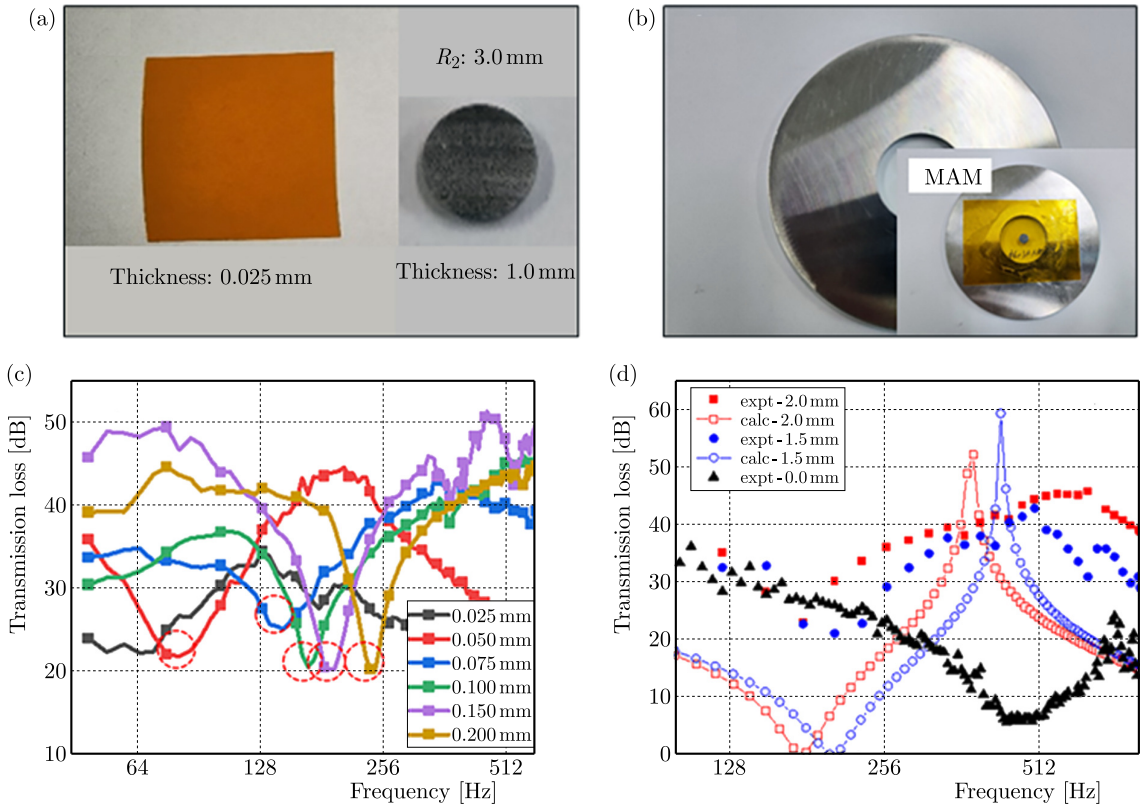

Fig. 4. Experimental results of thin-film acoustic metamaterials: (a) components of thin-film acoustic metamaterials; (b) the prepared acoustic metamaterial cell; (c) sound insulation test results of films of different thicknesses; (d) comparison of experimental and calculated results.

Experimental comparisons were conducted on six different thicknesses of films combined with five types of additional masses, as shown in Fig. 4c. It can be seen that with the increase of film thickness, the first-order resonance frequency (sound insulation valley frequency) of the structure increases. The increase of thin film thickness can be equivalent to the increase of structural stiffness, so that the first-order resonance frequency of the structure increases. On the other hand, increasing the thickness of additional mass enhances the overall equivalent mass of the structure, resulting in lower natural frequencies and shifting sound insulation valley frequencies towards lower frequencies.

By comparing theoretical and experimental data for MAMs and analyzing their design parameters such as film thickness, mass thickness, and radius on sound insulation curves, suitable design parameters are selected for addressing low-frequency noise issues inside high-speed train compartments. Focusing on frequencies below 500 Hz, a structure composed of a 2 mm thick additional mass combined with a 0.1 mm thick film is chosen after screening processes since its sound insulation curve exceeds 30 dB within 125 Hz–500 Hz range, as shown in Fig. 4d.

Incorporating this structure into flat panel noise reduction schemes showed improved sound insulation performance compared to traditional structures, as shown in Fig. 5a. Considering the problem of structural vibration transmission in the practical application process, the vibration state of the surface of the two structures is tested and compared, and there is almost no difference, as shown in Fig. 5b, indicating that the internal metamaterials had little influence on the vibration of the overall structure, and metamaterials mainly played a role in sound insulation.

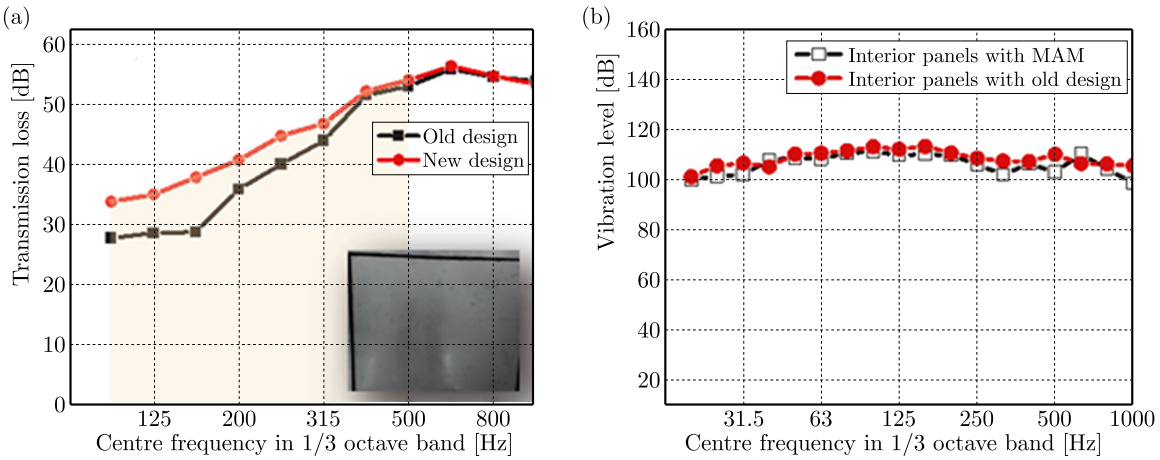

Fig. 5. Noise reduction comparison of different design schemes: (a) sound insulation comparison of design schemes with or without acoustic metamaterials; (b) structural surface vibration comparison of different schemes.

4. Conclusion

In this paper, the acoustic and vibration characteristics of MAMs were studied, leading to the following conclusions.

By designing the characteristics of low frequency sound insulation, a noise reduction structure of composite acoustic metamaterials was proposed to solve the problem of low frequency noise reduction inside high-speed EMUs.

Through theoretical analysis, it can be concluded that by adjusting parameters such as radius and surface density of additional mass as well as surface density of thin films, one can design structural sound insulation coefficients accordingly.

Experimental comparisons were conducted on six different thicknesses of films combined with five types of additional masses. The experimental results verified sound insulation performance of composite acoustic metamaterials. With the increase of film thickness, the first-order resonance frequency of the structure increases. Increasing the thickness of additional mass enhances the overall equivalent mass of the structure, resulting in lower natural frequencies and shifting sound insulation valley frequencies towards lower frequencies.

The MAMs analyzed in this research has already been studied for low frequency noise control. However, it has not been used in high-speed EMUs. The proposed composite acoustic metamaterials only consist of a single mass and a single film structure, which is simple in structure. The plane-type structure can be applied to areas such as vehicle floors, roofs, and side walls in the future. Due to its good acoustic performance, small thickness and mass, it has great potential for designing lightweight noise reduction structures in small design spaces, providing rich ideas for the noise reduction design of high-speed trains.

Acknowledgments

This work was supported by Research on Noise Characteristics of High-Speed EMU Running in Tunnel and Methods of Vibration and Noise Reduction (no. N2023J070), Research on

Vibration and Noise Performance of the EMU in the Middle and Late Life (no. 2021YJ306), Fundamental Research Funds for the Central Universities (no. 2022JBZY028), Science and Technology Research and Development Plan of China National Railway Group Corporation Limited (no. L2022Z002), and Beijing Natural Science Foundation (no. 3244035).

References

1. Ahluwalia, D.S., Kriegsmann, G.A., & Reiss, E.L. (1985). Scattering of low-frequency acoustic waves by baffled membranes and plates. *The Journal of the Acoustical Society of America*, *78*(2), 682–687. https://doi.org/10.1121/1.392437
2. Assouar, B., Oudich, M., & Zhou, X. (2016). Acoustic metamaterials for sound mitigation. *Comptes Rendus. Physique*, *17*(5), 524–532. https://doi.org/10.1016/j.crhy.2016.02.002
3. Fang, N., Xi, D., Xu, J., Ambati, M., Srituravanich, W., Sun, C., & Zhang, X. (2006). Ultrasonic metamaterials with negative modulus. *Nature materials*, *5*(6), 452–456. https://doi.org/10.1038/nmat1644
4. Ho, K.M., Cheng, C.K., Yang, Z., Zhang, X.X., & Sheng, P. (2003). Broadband locally resonant sonic shields. *Applied Physics Letters*, *83*(26), 5566–5568. https://doi.org/10.1063/1.1637152
5. Jena, D.P., Dandsena, J., & Jayakumari, V.G., (2019). Demonstration of effective acoustic properties of different configurations of Helmholtz resonators. *Applied Acoustics*, *155*, 371–382. https://doi.org/10.1016/j.apacoust.2019.06.004
6. Jung, J., Kim, H.G., Goo, S., Chang, K.J., & Wang, S. (2019). Realisation of a locally resonant metamaterial on the automobile panel structure to reduce noise radiation. *Mechanical Systems and Signal Processing*, *122*, 206–231. https://doi.org/10.1016/j.ymssp.2018.11.050
7. Kriegsmann, G.A., Norris, A., & Reiss, E.L. (1984). Acoustic scattering by baffled membranes. *The Journal of the Acoustical Society of America*, *75*(3), 685–694. https://doi.org/10.1121/1.390579
8. Liu, Z., Zhang, X., Mao, Y., Zhu, Y.Y., Yang, Z., Chan, C.T., & Sheng, P. (2000). Locally resonant sonic materials. *Science*, *289*(5485), 1734–1736. https://doi.org/10.1126/science.289.5485.1734
9. Lu, K., Wu, J.H., Guan, D., Gao, N., & Jing, L. (2016). A lightweight low-frequency sound insulation membrane-type acoustic metamaterial. *AIP Advances*, *6*(2), Article 025116. https://doi.org/10.1063/1.4942513
10. Ma, F., Wu, J.H., Huang, M., Fu, G., & Bai, C. (2014). Cochlear bionic acoustic metamaterials. *Applied Physics Letters*, *105*(21), Article 213702. https://doi.org/10.1063/1.4902869
11. Naify, C.J., Chang, C.M., McKnight, G., & Nutt, S.R. (2011). Transmission loss of membrane-type acoustic metamaterials with coaxial ring masses. *Journal of Applied Physics*, *110*(12), Article 124903. https://doi.org/10.1063/1.3665213
12. Naify, C.J., Chang, C.M., McKnight, G., & Nutt, S.R. (2012). Scaling of membrane-type locally resonant acoustic metamaterial arrays. *The Journal of the Acoustical Society of America*, *132*(4), 2784–2792. https://doi.org/10.1121/1.4744941
13. Rostami-Dogolsara, B., Moravvej-Farshi, M.K., & Nazari, F. (2016). Acoustic add-drop filters based on phononic crystal ring resonators. *Physical Review B*, *93*(1), Article 014304. https://doi.org/10.1103/PhysRevB.93.014304
14. Sheng, P., Zhang, X.X., Liu, Z., & Chan, C.T. (2003). Locally resonant sonic materials. *Physica B: Condensed Matter*, *338*(1–4), 201–205. https://doi.org/10.1016/S0921-4526(03)00487-3
15. Song, Y., Feng, L., Wen, J., Yu, D., & Wen, X. (2015). Reduction of the sound transmission of a periodic sandwich plate using the stop band concept. *Composite Structures*, *128*, 428–436. https://doi.org/10.1016/j.compstruct.2015.02.053
16. Thompson, D. & Gautier, P.-E. (2006). Review of research into wheel/rail rolling noise reduction. *Proceedings of the Institution of Mechanical Engineers, Part F: Journal of Rail and Rapid Transit*, *220*(4), 385–408. https://doi.org/10.1243/0954409JRRT79

17. Thompson, D.J., Latorre Iglesias, E., Liu, X., Zhu, J., & Hu, Z. (2015). Recent developments in the prediction and control of aerodynamic noise from high-speed trains. *International Journal of Rail Transportation*, *3*(3), 119–150. https://doi.org/10.1080/23248378.2015.1052996

18. Varanasi, S., Bolton, J.S., Siegmund, T.H., & Cipra, R.J. (2013). The low frequency performance of metamaterial barriers based on cellular structures. *Applied Acoustics*, *74*(4), 485–495. https://doi.org/10.1016/j.apacoust.2012.09.008

19. Wang, Z. & Choy, Y. (2019). Acoustical coupling and radiation control of open cavity using an array of Helmholtz resonators. *Mechanical Systems and Signal Processing*, *130*, 632–648. https://doi.org/10.1016/j.ymssp.2019.05.037

20. Yoshizawa, T., Mochida, T., & Yamazaki, T. (2019). Study of analysis method of interior noise in railway cars by means of ray tracing method. *Mechanical Engineering Journal*, *6*(5), Article 18-00449. https://doi.org/10.1299/mej.18-00449

21. Zhang, Y., Wen, J., Zhao, H., Yu, D., Cai, L., & Wen, X. (2013). Sound insulation property of membrane-type acoustic metamaterials carrying different masses at adjacent cells. *Journal of Applied Physics*, *114*(6), Article 063515. https://doi.org/10.1063/1.4818435

22. Zhou, G., Wu, J., Lu, K., Tian, X., Liang, X., Huang, W., & Zhu, K. (2019). An approach to broaden the low-frequency bandwidth of sound insulation by regulating dynamic effective parameters of acoustic metamaterials. *Journal of Physics D: Applied Physics*, *52*(21), Article 215102. https://doi.org/10.1088/1361-6463/ab07f9

Manuscript received August 3, 2024; accepted for publication January 13, 2025; published online March 25, 2025.